Ice Surface and Bed Roughness Estimation of Petermann Glacier

Manjish Adhikari, Jilu Li
The Center for Remote Sensing of Ice Sheets (CReSIS), University of Kansas, Lawrence, KS, USA

***Abstract*— Understanding the subglacial conditions is crucial in determining the ice dynamics and predicting the stability of ice sheets. Radio echo sounding (RES) survey have been extensively used to map the ice sheets on Greenland and Antarctica. Using RES data, basal conditions of ice sheets can be determined from estimated reflectivity that is affected by ice surface and bed roughness. Roughness is also one of the important parameters to explain ice dynamics. In this paper the ice surface and bed roughness of Petermann glacier, one of the largest outlet glacier of Greenland, is determined using Multi Channel Coherent Radar Depth Sounder (MCoRDS) data following Grima's method of statistical fitting of echo amplitudes. The roughness derived from MCoRDS is compared and verified with the roughness estimations from Airborne Topographic Mapper (ATM)and Ku-band altimeter measurements. It has been observed that Petermann glacier has rougher ice inland and a smoother bed towards the trunk of the glacier.**

Keywords— remote sensing, radio echo sounding, Ice basal condition and reflectivity

I. INTRODUCTION

With the global climate change and temperature rise there's constant effect on the polar ice sheet thus making significant change in the rise of sea level. Huge efforts have been made to study the ice sheet conditions especially the Antarctic and Greenland ice sheets. Ice sheet dynamics play an important role in explaining the glaciers and melting. Ice motion is affected by two main factors i.e. temperature and the strength of the bases [1]. Understanding the subglacial environment or basal conditions is important to predict the stability of ice sheet as basal lubrication threatens the stability of ice sheet.

RES have been extensively used in polar surveys. The data collected by these radars have been used to understand ice dynamics and subglacial conditions. Based on the radar signal intensity from the ice bed, distinctions between basal water and rocks can be made [1] where strong ice bed reflections correspond to basal melt. Certain subglacial lakes have been identified both in Greenland and Antarctica [3,4,5]. However, the ice bed reflectivity first needs to be properly compensated for the geometrical spreading loss, ice attenuation, and rough surface scattering. To calculate the bed reflectivity, the effects of rough beds need to be compensated for otherwise frozen beds may be misidentified as basal melts due to higher reflectivity.

Bed roughness is also one of the important basal parameters that can explain ice dynamics [6]. Bingham and Siegert, 2009 present two examples from West Antarctica, which demonstrate the utility of bed roughness in determining the presence and extent of subglacial sediments, glacial dynamics and former ice-sheet size [7]. Fast flowing ice corresponds to a smoother bed and slower to rougher beds [8,16]. The changes of the ice sheet conditions are being monitored by flying missions over the same place in certain time period. One of the changes that can be identified is the change in the surface roughness that can show the changing nature of ice dynamics at that place.

Roughness can be estimated from RES data using different methods like Fast Fourier transforms [9], Integral Equation Model [10] and statistical method [11]. The MCoRDS radar used by the Center for Remote Sensing of Ice sheets (CReSIS) for polar surveys can penetrate deep into ice sheets to reveal ice bottoms and the backscattered signal from the bed [13,14]. These bed echoes are analyzed to understand the basal conditions [1,15]. We apply Grima's approach to derive roughness of the ice bed and ice surface, which can be used to model ice bed reflectivity and understand basal conditions.

Roughness is a function of the radar system parameters as it varies with the wavelength of the radar signal. Roughnesses calculated by the MCoRDS [13] are compared with that of laser altimeter by ATM group [17] and Ku Band altimeter [19]. However, RMS height is an inherent property of the system parameters [20] hence these systems are expected to have quantitatively different results but qualitatively similar results, which gives us confidence towards the calculation of ice bed reflectivity. Laser altimeter and Ku-band maps only the ice surface hence here we compare the surface RMS heights calculated from these three systems.

Peterman glacier is one of the rapidly changing outlet glaciers in Northern Greenland that drains more than 4% of the total ice sheet. Two huge glacier calving events have occurred at Petermann Glacier over the past 5 years, one in 2010 and another in 2012 [22, 23]. Petermann glacier has the second-longest floating ice shelf in Greenland with a permanent floating ice tongue [24,25], and flows with an average velocity of just over 1 km per annum [22]. To study the basal conditions of Petermann glacier, roughness is an important component which is studied in this paper.

II. METHODOLOGY

A. Data Collection

The Center for Remote Sensing of Ice Sheets (CReSIS) deployed airborne Multi Channel Coherent Radar Depth Sounder (MCoRDS), a nadir looking radar mounted on an aircraft flying usually at the height of 500 meters from the ice

surface to map the thickness of Greenland and Antarctica ice sheets in NASA's Operation Ice Bridge (OIB) missions [13,19]. This analysis studies the surface roughness of Peterman Glacier, which was mapped using MCORDS in 2010-2014 [14].

MCoRDS operates with linear chirp waveform within the frequency band from 180 MHz to 210 MHz. It usually has six transmit channels and receivers to allow beamforming during data processing. An Arbitrary waveform generator (AWG) is used to generate the waveforms which is pre-stored in digital form and converted to analog form using a D/A converter [6]. Three different pulses are used. The short pulses of 1 µs and 3 µs are used to detect the surface and shallow ice layers and doesn't have high penetration power whereas 10-µs pulse is better in detecting the ice bed as it has higher penetration power. The short and long pulses are alternatively sent with time division multiplexing at pulse repetition frequency of 12 KHz. The received signals are digitized using A/D converters at sampling rate of 111MHz or 150 MHz with 14 ADC bits. Table I. describes some basic radar system parameters.

TABLE I. SYSTEM PARAMETERS

Description	**Characteristic**
Center Frequency	195 MHz
Bandwidth	180-210 MHz
Transmit Signal Type	Linear Up Chirp
Transmit Power	1050 W
Signal Duration	1 µs and 10 µs (Low Altitude) 30 µs (High Altitude
Transmit Channels	7
Receive Channels	16
Noise Figure	2
Sampling Rate	111 MHz
ADC Bits	14
Dynamic Range	Waveform Playlist
Data Rate	32 MB/sec per channel

The complex data received after processing from this radar has along track resolution of about 0.5 m which is surface tracked in the echogram-using the tracker developed by CReSIS to derive the surface echo amplitudes.

The surface illuminated by the radar or its footprint is important is deriving the surface roughness. For any radar, the footprint bounded by compressed pulse length is given by [11]:

$$D_{PL} = 2\sqrt{\frac{hc}{\Delta f}} \qquad (1)$$

where 'h' is the height of the aircraft from the surface, Δf is the bandwidth of the radar signal. For MCoRDS, the flying height is typically 500 meters and the bandwidth being 30 MHz the radar footprint thus averages around 141 meters for ice surface and for average ice depth of 2000 meters, the footprint is around 316 meters. Surface roughness can be characterized by root mean square height σ_h and correlation length (L_c) but recent studies derive L_c directly from σ_h with insitu instrumentations [20]. The echo amplitudes of the surface and ice bed are fitted using rice distribution for every 200 m with overlapping of every 100m to calculate the coherent and incoherent powers and then from power statistics, derive the RMS height of the surface [11].

Surface roughness calculations are also made from the Airborne Topographic Mapper (ATM), a conical scanning airborne laser developed at NASA Wallops Flight Facility to monitor the earth's topography. ATM measures the surface elevation based on the two-way travel time of laser pulses along with the differential GPS and aircraft attitude information. It operates at 532 nm with a pulse repetition frequency of 5 kHz and a scan rate of 20 Hz [18]. The along-track resolution is 3-4 m with laser footprint of ~1m. The primary data product of ATM is QFIT, which is dense surface elevation measurements. It is condensed into ICESSN which fits a plane to the block of points selected at regular intervals (0.5 sec) along track with overlapping of 50% between successive blocks [17]. It also measures the South-North and West-East slope for the plane and RMS fit of the ATM data to the plane. The radar lines of MCoRDS coincide with the track 0 of ICESSN data. ICESSN data has along-track resolution of 80 meters and hence the RMS height from this laser system is calculated by the interpolation for the corresponding radar locations.

In addition, Operation IceBridge missions also employ the Ku-band Altimeter developed by CReSIS which is an Ultra Wideband Frequency (UWB) Modulated Continuous wave (FMCW) radar operating usually from 12-18 GHz [19]. It provides high precision surface elevation measurements over polar ice sheets. The along-track resolution of the data from Ku-band is 0.2 meters after hardware presums.

B. Theory and Data Processing

Reflection and scattering of EM waves are affected by the roughness of the surface. From specular surfaces the received field is coherent with known phase given by $E = A\, e^{j\varphi_0}$ whereas from rough surfaces they are scattered with unknown phase called the incoherent components[26]. Both the coherent and incoherent components contribute to the total signal received at the radar receiver, which can be written as:

$$E = e^{j\varphi_0} + \sum_{i=1}^{N} A e^{j\varphi_i} \qquad (2)$$

where the first part is the coherent component and the second part is the incoherent component of the power received at the radar receiver. The balance between these two is a function of surface roughness [11].

Grima, 2012 proposed a statistical method in which the coherent and incoherent components can be extracted by the statistical fitting of the received amplitude envelopes [12]. The received power can be assumed to be due the summations of power scattered from N random elements, each with a certain phase differences 'φ'. Different envelope methods can be applied to the 'N' random echo amplitudes to estimate surface characteristics but the domain of validity is different for

different types of fittings. Grima uses the homodyne K-distribution to model the surface which is valid even at the limiting case, however, it does not have a closed form and is difficult to solve [11]. Specular surfaces tend to correlate with Rician fitting while rougher surfaces correlate with K-noise statistics. The ice surface and bed echo amplitude here are fitted with the Rician distribution as the domain of validity of Rician distribution fitting is large. The Rician distribution fitting fails only when 'N', reflectors population in footprint, is a random variable with a negative binomial distribution. The Rician distribution is given by

$$P(A|a,s) = \frac{A}{s^2} e^{-\frac{A^2+a^2}{2s^2}} I_0\left(\frac{aA}{s^2}\right) \quad (3)$$

for interval [a, ∞] where $I_0(z)$ is the modified Bessel function of first kind with zero order and 'a' and 's' are the shape parameters. From the Rician fitting, the coherent and incoherent power are obtained as:

$$P_c = a^2 \quad (4)$$
$$P_n = 2\,s^2 \quad (5)$$

The ratio of coherent and the incoherent power is related to the RMS height as [11]

$$\frac{P_c}{P_n} = \frac{e^{-(2k\sigma_h)^2}}{4k^2{\sigma_h}^2} \quad (6)$$

where $k = \frac{2\pi}{\lambda}$ is the wave number. Coherent power 'P_c' and incoherent power 'P_n' derived from the statistical power distribution fitting are used in equation 10 to derive the RMS height σ_h for the radar.

The radar lines of MCoRDS coincide with the track 0 of ICESSN data. ICESSN data has along track resolution of 80 meters and hence the RMS height from this laser system is calculated by the interpolation for the radar locations.

Similarly based on the surface altitudes obtained from Ku-Band, RMS height was calculated from the Ku-band altimeter by using samples every 200 m with 50% overlapping as:

$$\sigma_h = \sqrt{\frac{1}{n}\sum_{i=1}^{n}(z_i - \bar{z}_i)^2} \quad (7)$$

Roughness causes the reduction in received power by [4,27]

$$\rho = e^{-\sigma_\emptyset^2} I_0^2\left(\frac{\sigma_\emptyset^2}{2}\right) \quad (8)$$

where I_0 is zeroth order modified Bessel function of first kind, $\sigma_\emptyset$ is the phase variation due to surface roughness given by [28].

$$\sigma_\emptyset = \frac{4\pi\sigma_h}{\lambda}\left(\sqrt{\varepsilon} - 1\right) \quad (9)$$

The correction ρ is applied to each survey line in order to compensate for the losses due to rough surface.

III. RESULTS

The radar data used for analysis was collected by CReSIS using MCoRDS in 2010-2014 season in Greenland. The particular segment 20141026_02 from Antarctica, as shown in the red box in Fig.1, is used to analyze the validity of this method because of the good quality of data, and variable surface roughness as seen from the Ku-band altimeter in Fig. 2. Areas with smooth surface can be seen in Fig. 2.a and rougher surface from Fig. 2.b with their corresponding Ku-band radar echograms on 2.c and 2.d.

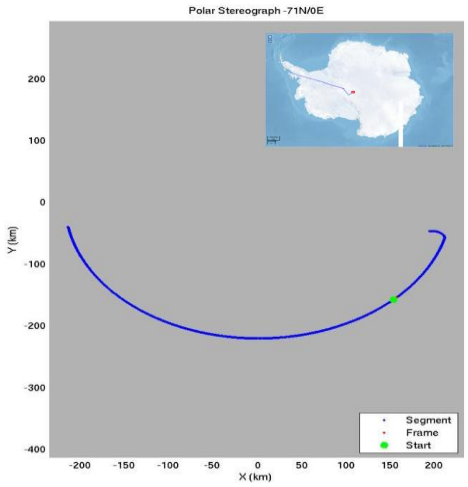

Fig. 1. Area used for Roughness Calculation

Here the echo amplitudes of around 500 samples (i.e. 200 m along track) are fit to the Rician distribution to derive the surface RMS height using MATLAB. For validation of the RMS height derived from MCoRDS using Grima's method [11], the RMS height was also derived for the corresponding radar locations using laser data. Figure 3 shows the comparison between the surface roughness measurements obtained from three systems, red indicating radar, blue indicating laser and green indicating Ku-band measurements. It can be clearly observed that the RMS height calculated corresponds to the surface features seen in the Ku-Band altimeter image. The rougher surface features from the echogram coincide with the corresponding higher value of RMS height whereas same for the comparatively smoother surfaces of lower RMS value.

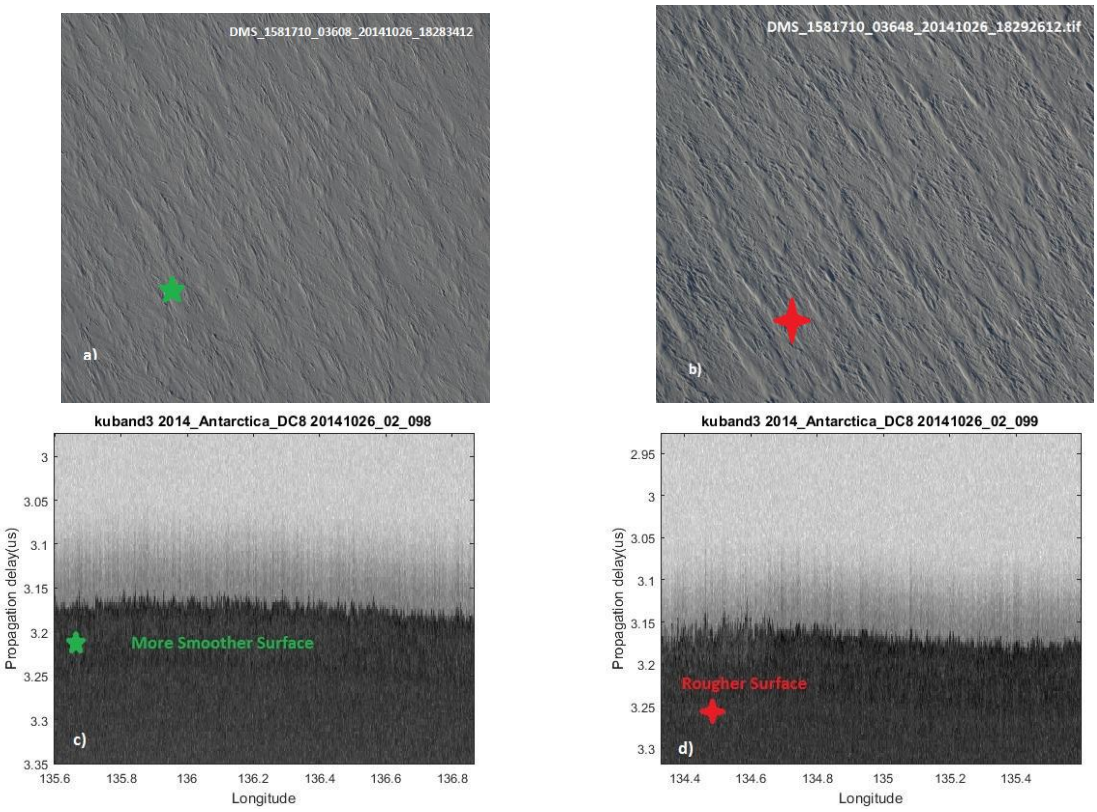

Fig.2. DMS pictures of areas with Smoother (a) and Rougher (b) Surfaces [30]. Radar Echograms obtained from Ku-Band Altimeter showing corresponding smooth (a) and rough areas (b) [14]

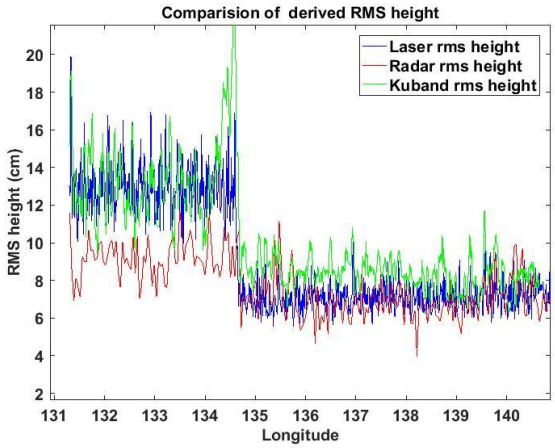

Fig. 3. Surface RMS heights obtained from MCoRDS (red), ATM (blue) and Ku-Band Altimeter (green)

It can be distinguished that the areas with higher RMS in laser data are also seen rough by the radar however there's a certain bias which can be owed to the facts that these are two different systems operating with different system parameters and ground surface roughness being the inherent property of radar specifications [20]. The RMS heights detected by radar is bounded because this uses power statistics and signal components fade and become undetectable with increasing roughness [11]. In addition to this, the data obtained by Ku-Band of CReSIS analyzed for the corresponding frames yielded similar results.

Following this method, it was used to determine the surface and bed roughness of Peterman Glacier, which can be later used to model the ice bed reflectivity. The radar lines extend from inland towards the ice margin as well as cross lines and extending from east to west as vertical lines. Straight lines are chosen as there's no loss due to aircraft banking.

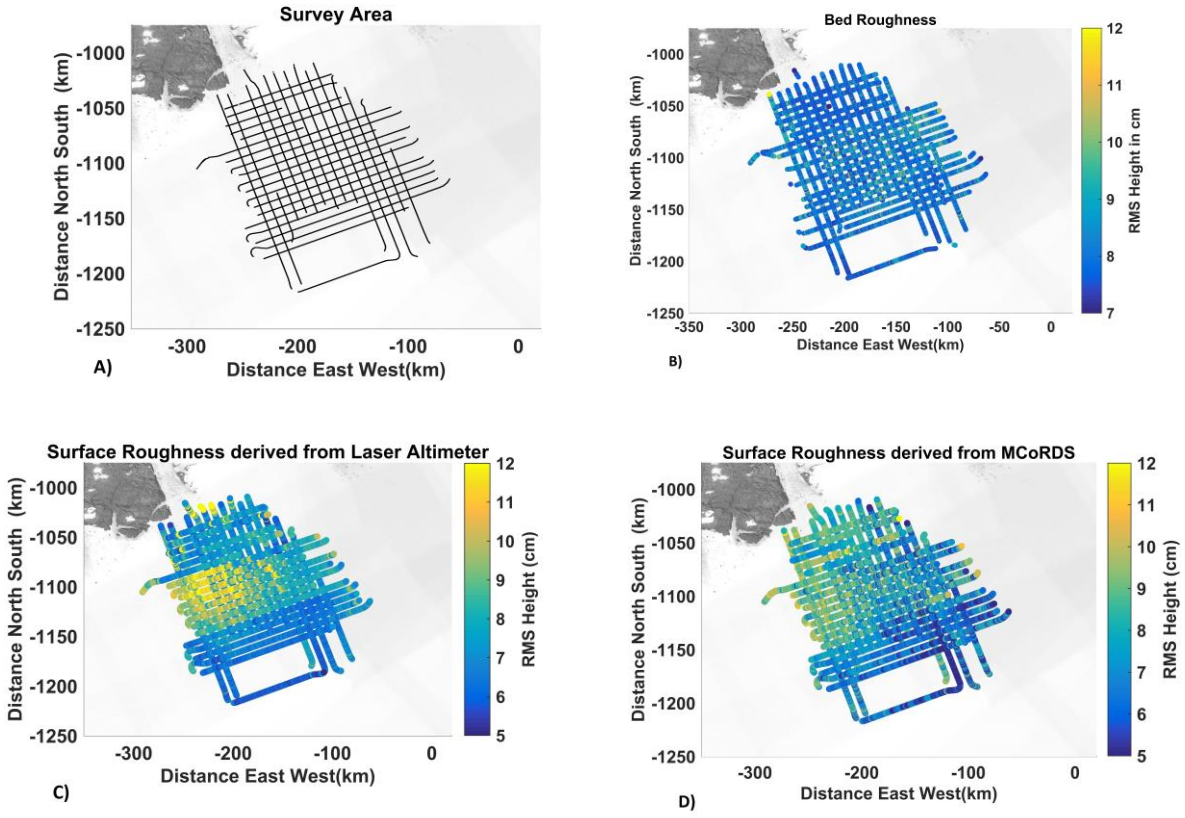

Fig. 4. Radar Survey area of Petermann Glacier under Operation IceBridge (A), Bed Roughness calculated from MCoRDS (B), Surface Roughness calculated from MCoRDS (C), Surface Roughness calculated from ATM (D),

The surface roughness for Peterman glacier was obtained using radar data and laser data as in Fig. 4. Ku- Band data are not available for this complete dataset hence not presented, however are cross-checked whenever available. Cross over analysis was done for obtained roughness which has 75% of the RMS height difference within ±2 cm. The results reveal that the surface roughness is greater towards the coastline, which is expected since the ice flow is obstructed at the coastline due to narrow passage. Higher RMS height values are seen towards the Northwest area. The difference between the radar derived RMS heights and laser derived RMS heights is within ±5 cm (99%) for the survey area. Fitting errors maybe introduced when RMS height is fit into equation 6 so it should be checked for convergence. Some of the errors to this method may also result from the surface and bottom tracking errors but automatic surface tracking method employed here decreases this type of errors. Also when the slope of the surface and roll of the aircraft is large then surface power is decreased hence constraints are applied on the roll and slope to minimize such errors. Areas with very high surface elevation changes have been removed since the surface stationarity isn't maintained.

In contrast, the bed roughness shows that the RMS height is lower towards the trunk of the glacier. Petermann Glacier lies in a deep subglacial trough, flanked by steep valley sides so it is fed by large area of ice sheet [8]. The flow rate is higher towards the margin of the glacier [Joughin et. Al 2010]. In situ erosion of the base or marine sediments filling the bedrock gaps might have caused the bed to be smoother towards the trunk of the glacier. Petermann is one of the largest outlet glaciers hence more detail analysis is needed for further conclusions.

CONCLUSION AND FUTURE WORK

We estimated the ice surface and bed roughness of Petermann catchment area using a statistical method fitting the echo amplitudes of MCoRDS radar operating at VHF band. We verified the method by comparing roughness estimates from laser altimeter and Ku-Band altimeter measurements. We also obtained roughness characteristics of Peterman Glacier that are correlated with the ice bed topography and ice flow dynamics and that will be used next to constrain the ice bed reflectivity to infer the glacier's basal condition.

ACKNOWLEDGMENT

This work is supported by NASA Grant # NNX14AL99G. The Petermann Glacier surveys were funded by NASA Grant #NNX10AT68G. We gratefully acknowledge the contributions of staff, faculty and students at CReSIS.

REFERENCES

[1] Oswald, G., & Gogineni, S. (2008). Recovery of subglacial water extent from Greenland radar survey data. Journal of Glaciology, 54(184), 94-106. doi:10.3189/002214308784409107

[2] Robin, G.de Q., C.W.M. Swithinbank and B.M.E. Smith. 1970. Radio echo exploration of the Antarctic ice sheet. IASH Publ. 86 (Symposium at Hanover 1968 – Antarctic Glaciological Exploration (ISAGE)), 97–115

[3] Oswald, G.K.A. and G.de Q. Robin. 1973. Lakes beneath the Antarctic ice sheet. Nature, 245(5423), 251–254

[4] Peters, M.E., D.D. Blankenship and D.L. Morse. 2005. Analysis techniques for coherent airborne radar sounding: application to West Antarctic ice streams. J. Geophys. Res., 110(B6), B06303. (10.1029/2004JB003222.)

[5] Siegert, M., Carter, S., Tabacco, I., Popov, S., & Blankenship, D. (2005). A revised inventory of Antarctic subglacial lakes. Antarctic Science, 17(3), 453-460. doi:10.1017/S0954102005002889

[6] Bingham, R. G., and M. J. Siegert (2007), Radar-derived bed roughness characterization of Institute and Möller ice streams, West Antarctica, and comparison with Siple Coast ice streams, Geophys. Res. Lett., 34, L21504, doi:10.1029/2007GL031483.

[7] Robert G. Bingham, Martin J. Siegert, Quantifying subglacial bed roughness in Antarctica: implications for ice-sheet dynamics and history, In Quaternary Science Reviews, Volume 28, Issues 3â€“4, 2009, Pages 223-236, ISSN 0277-3791, https://doi.org/10.1016/j.quascirev.2008.10.014.

[8] Rippin, D. (2013). Bed roughness beneath the Greenland ice sheet. Journal of Glaciology, 59(216), 724-732. doi:10.3189/2013JoG12J212

[9] Justin Taylor, Martin J. Siegert, Antony J. Payne, Bryn Hubbard, Regional-scale bed roughness beneath ice masses: measurement and analysis, In Computers & Geosciences, Volume 30, Issue 8, 2004, Pages 899-908, ISSN 0098-3004, https://doi.org/10.1016/j.cageo.2004.06.007.

[10] A. K. Fung and K. S. Chen "An update on the IEM surface backscattering model " IEEE Geosci. and Remote Sens. Lett. vol. 1 (2) pp. 75-77 2004

[11] Cyril Grima, Dustin M. Schroeder, Donald D. Blankenship, 2014, Duncan A. Young, Planetary landing-zone reconnaissance using ice-penetrating radar data: Concept validation in Antarctica, Planetary and Space Science, 103:191–204

[12] C. Grima, W. Kofman, A. Herique, et al. Quantitative analysis of Mars surface radar reflectivity at 20 MHz Icarus, 220 (2012), 10.1007/s11214-012-9916-y

[13] Rodríguez-Morales, F., et al. (2014), Advanced multifrequency radar instrumentation for polar research, IEEE Trans. Geosci. Remote Sens., 52(5), 2824–2842, doi:10.1109/TGRS.2013.2266415.

[14] Leuschen, Carl, Prasad Gogineni, Richard Hale, John Paden, Fernando Rodriguez, Ben Panzer, Daniel Gomez. 2014, updated 2016. IceBridge MCoRDS L1B Geolocated Radar Echo Strength Profiles, Version 2

[15] Santhosh Kumar Malyala, Jilu Li, Manjish Adhikari, Fernando Rodriguez Morales. "Estimation of ice basal reflectivity of Byrd glacier using RES data," 2017 IEEE International Geoscience and Remote Sensing Symposium.

[16] Rippin, D., Vaughan, D., & Corr, H. (2011). The basal roughness of Pine Island Glacier, West Antarctica. Journal of Glaciology, 57(201), 67-76. doi:10.3189/002214311795306574

[17] Studinger, M. S. 2014, updated 2017. IceBridge ATM L2 Icessn Elevation, Slope, and Roughness. Version 2. [2012-2014]. Boulder, Colorado USA: NASA DAAC at the National Snow and Ice Data Center. http://dx.doi.org/10.5067/CPRXXK3F39RV. [2017].

[18] Kwok, R., G. F. Cunningham, S. S. Manizade, and W. B. Krabill (2012), Arctic sea ice freeboard from IceBridge acquisitions in 2009: Estimates and comparisons with ICESat, J. Geophys. Res., 117,

[19] S. Gogineni, J.-B. Yan, D. Gomez-Garcia, F. Rodriguez-Morales, C. Leuschen, Z. Wang, J. Paden, R. Hale, E. Arnold, D. Braaten, "Ultra-wideband radars for measurements over ICE and SNOW", Geoscience and Remote Sensing Symposium (IGARSS) 2015 IEEE International, pp. 4204-4207, 2015.

[20] N. Baghdadi, C. King, A. Chanzy, J. P. Wigneron, "An empirical calibration of the integral equation model based on SAR data soil moisture and surface roughness measurement over bare soils", Int. J. Remote Sens., vol. 23, no. 20, pp. 4325-4340, 2002.

[21] O. M. Johannessen, M. Babiker, M. W. Miles, Unprecedented retreat in a 50-year observational record for Petermann Glacier, North Greenland, Atmospheric and Oceanic Science Letters 6 (5) (2013) 259-265.

[22] Nick, F., Luckman, A., Vieli, A., Van Der Veen, C., Van As, D., Van De Wal, R., . . . Floricioiu, D. (2012). The response of Petermann Glacier, Greenland, to large calving events, and its future stability in the context of atmospheric and oceanic warming. Journal of Glaciology, 58(208), 229-239. doi:10.3189/2012JoG11J242

[23] K. K. Falkner, H. Melling, A. M. Münchow, J. E. Box, T. Wohlleben, H. L. Johnson, P. Gudmandsen, R. Samelson, Copland, K. Steffen, E. Rignot, A. K. Higgins, Context for the Recent Massive Petermann Glacier Calving Event, Eos, Transactions American Geophysical Union 92 (14) (2011) 117-118. doi:10.1029/2011EO140001.

[24] Rignot E, Gogineni S, Joughin I and Krabill W (2001) Contribution to the glaciology of northern Greenland from satellite radar interferometry. J. Geophys. Res., 106(D24), 34 007–34 019

[25] Moon T and Joughin I (2008) Changes in ice front position on Greenland's outlet glaciers from 1992 to 2007. J. Geophys. Res., 113(F2), F02022 (doi: 10.1029/2007JF000927)

[26] Ulaby, F.T.,Moore,R.K.,Fung,A.K.,1982. Radar Remote Sensing and Surface Scattering and Emission Theory, Microwave Remote Sensing Active and Passive

[27] Boithias, L., 1987, Radiowave propagation: McGraw-Hill

[28] Dustin M. Schroeder, Cyril Grima, and Donald D. Blankenship (2016). "Evidence for variable grounding-zone and shear-margin basal conditions across Thwaites Glacier, West Antarctica." GEOPHYSICS, 81(1), WA35-WA43.https://doi.org/10.1190/geo2015-0122.1

[29] Joughin I, Smith B, Howat IM, Scambos T and Moon T (2010) MEaSUREs Greenland ice sheet velocity map from InSAR data. National Snow and Ice Data Center, Boulder, CO. Digital media: http://nsidc.org/data/docs/measures/nsidc0478_joughin

[30] Dominguez, R. 2010, updated 2017. IceBridge DMS L1B Geolocated and Orthorectified Images, Version 1. [2014]. Boulder, Colorado USA. NASA National Snow and Ice Data Center Distributed Active Archive Center. doi: http://dx.doi.org/10.5067/OZ6VNOPMPRJ0. [2016].